Electronic Supplementary Material (ESI) for Journal of Materials Chemistry C.
This journal is © The Royal Society of Chemistry 2024

SUPPORTING INFORMATION

Hansen Solubility Approach Towards Green Solvent Processing:

N-Channel Organic Field-Effect Transistors in Ambient

Ibrahim Deneme, Tevhide Ayça Yıldız, Nilgun Kayaci, Hakan Usta*

Department of Nanotechnology Engineering, Abdullah Gül University, 38080 Kayseri, Turkey.

* Address correspondence to: Prof. Hakan Usta (hakan.usta@agu.edu.tr)

Table S1. The molecular structures, OFET device configurations/performances, semiconductor thin-film deposition methods, and the green solvents employed during deposition for previously reported solution-processable *n*-type and *p*-type semiconductors. The abbreviated names for each molecular structure are presented as indicated in their respective references.

Molecular Structure	Solution-based deposition method	Green Solvent	OFET Performance I_{on}/I_{off}, μ($cm^2/V{\cdot}s$), V_{th}(V)	OFET Device Configuration	OFET Character. Environment	References
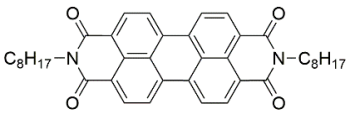 **PTCDI-C_8**	Solution-shearing	Anisole	1.5×10^7, 0.13, 36 (*n*-channel)	Si/SiO_2/PS-brush/**PTCDI-C_8**/Au	Vacuum	*Ho et al.*[1]
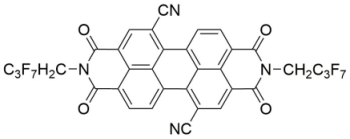 **PDIF-CN_2**	Solution-shearing	Purasolv EHL	2.3×10^3, 0.069, -32 (*n*-channel)	Si/SiO_2/PS-brush/**PDIF-CN_2**/Au	Vacuum	
		Methyl laurate	1.3×10^2, 0.000094, -52 (*n*-channel)			
		n-Amyl acetate	3.4×10^2, 0.000010, -52 (*n*-channel)			

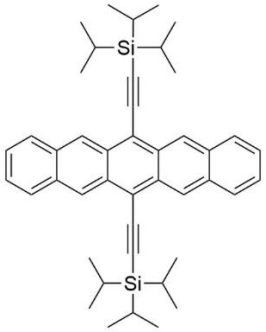 **TIPS-PEN**	Solution-shearing	t-Amyl methyl ether	5.1×10^{4}, 1.40, -32 (*p*-channel)	Si/SiO_2/PS-brush/**TIPS-PEN**/Au	Vacuum	Ho *et al.*[1]
		Anisole	4.4×10^{5},1.90, -33 (*p*-channel)			
		Isopropyl acetate	2.2×10^{4},0.67, -33 (*p*-channel)			
		Isobutyl acetate	3.7×10^{4}, 2.6, -29 (*p*-channel)			
		Dimethyl Carbonate	4.6×10^{4}, 1.3, -25 (*p*-channel)			
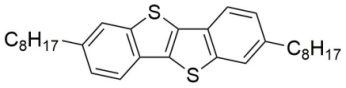 **C_8-BTBT**	Solution-shearing	t-Amyl methyl ether	$3.5\times10^{8,}$ 0.73, -30 (*p*-channel)	Si/SiO_2/PS-brush/**C_8-BTBT**/Au	Vacuum	
		Isobutyl acetate	4.6×10^{6}, 0.057, -31 (*p*-channel)			
		Isopropyl acetate	2.0×10^{8}, 0.92, -56 (*p*-channel)			
		Dimethyl Carbonate	2.3×10^{6}, 0.031, -19 (*p*-channel)			
		Anisole	1.1×10^{7}, 0.92, -38 (*p*-channel)			

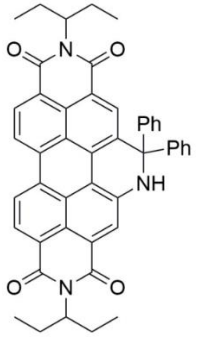 **X1**	Spin-coating	Propanol/n-butylamine	NA, 10^{-5},10 (*n*-channel)	Si/SiO_2/OTCS/**X1**/Au	Vacuum	Harris *et al.*[2]
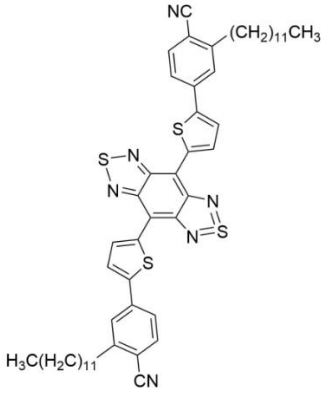 **TU-3**	Solution-shearing	Chlorobenzene/ diethyl succinate	6.43×10^4-2.84×10^5, 0.13-0.33, 0.2-4 (*n*-channel)	Si/SiO_2/PS-brush/**TU-3**/Au	Vacuum	Lee *et al.*[3]

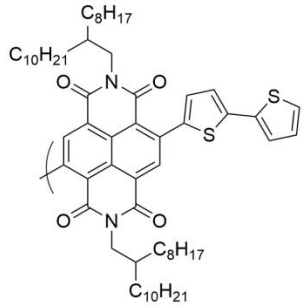 **P(NDI2OD-T2)**	Spin-coating	Chloroform/2-methyl tetrahydro furan	1.05-1.25×10^4, 0.086-0.11, 1.6-1.9 (*n*-channel)	Si/SiO_2/PS-brush/**P(NDI2OD-T2)**/Au	Vacuum	Lee *et al.*[3]
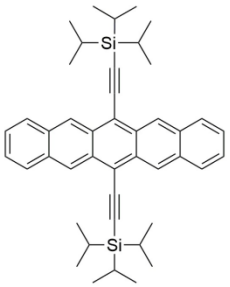 **TIPS-pentacene**	Solution-shearing	Toluene/ n-amyl acetate	1.67-3.31×10^7, 1.71-2.61, -23-(-16) (*p*-channel)	Si/SiO_2/PS-brush/**TIPS-pentacene**/Au	Vacuum	
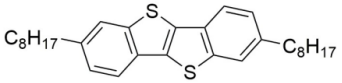 **C_8-BTBT**	Solution-shearing	Chloroform/2-methyl tetrahydro furan	2.85-9.81×10^7, 1.84-2.10, -30 (*p*-channel)	Si/SiO_2/PS-brush/**C_8-BTBT**/Au	Vacuum	

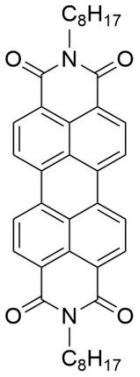 **PTCDI-C_8**	Solution-shearing	Anisole	$(1.5 \pm 0.7)\times10^5$, 0.31, 29±0.7 (*n*-channel)	Si/SiO_2/Shellac/**PTCDI-C_8**/Au	Vacuum	Lee *et al.*[4]
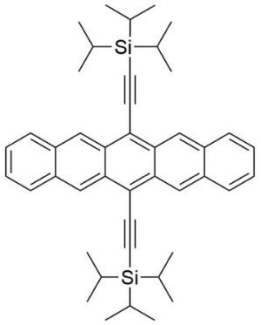 **TIPS-pentacene**	Solution-shearing	Tert-amyl methyl ether	$(7.0\pm3.5)\times10^6$, 0.61, -31±2.3 (*p*-channel)	Si/SiO_2/Shellac/**TIPS-pentacene**/Au	Vacuum	
		Isobutyl acetate	$(19\pm9.1)\times10^6$, 1.52, -30±3.8 (*p*-channel)			
		Anisole	$(4.0\pm2.5)\times10^6$, 1.11, -25±8.0 (*p*-channel)			

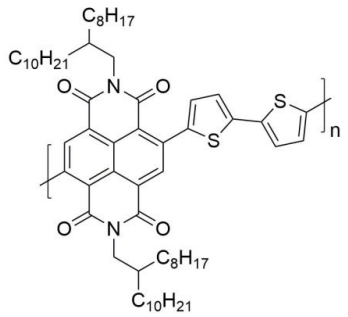 **P(NDI2OD-T2)**	Solution-shearing	Propylene glycol methyl ether acetate / 1,2-dichlorobenzene	NA, 0.28-1.03, 26.8-31.8 (*n*-channel)	Glass/Au-Ni/**P(NDI2OD-T2)**/PMMA/Al	Under N_2	Opoku *et al.*[5]
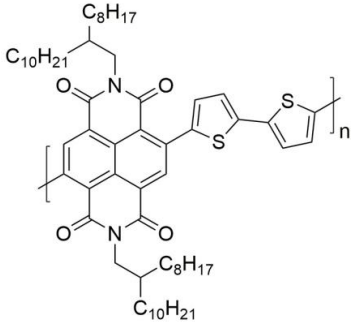 **P(NDI2OD-T2)**	Solution-shearing	Mesitylene/ acetophenone	$1.23\text{-}2.83\times10^3$, 0.448-0.574, 19.8-20.6 (*n*-channel)	Glass/Au-Ni/**P(NDI2OD-T2)**/ PMMA/Al	Under N_2	Opoku *et al.*[6]

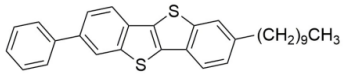 **Ph-BTBT-C$_{10}$**	Solution-shearing	Anisole	10^4-10^5, 0.01-3.96, -23-(-5) (*p*-channel)	Si/SiO$_2$/PS-brush/**Ph-BTBT-C$_{10}$**/Au	Vacuum	Yun *et al.*[7]
		Cyclohexanone	10^4-10^9, 0.01-5.07, -16-(-6) (*p*-channel)			
		Diethyl Carbonate	10^5-10^9, 0.04-3.22, -18-(-6) (*p*-channel)			
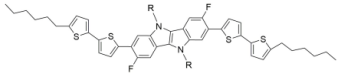 **PEG-IDIDF**	Solution-shearing	Ethanol-water	10^3-10^6, 5.53×10^{-4}-2.01×10^{-3}, (-1±4)-(1±3) (*p*-channel)	Si/SiO$_2$/PVN/**PEG-IDIDF**/Au	Under N_2	Hong *et al.* [8]

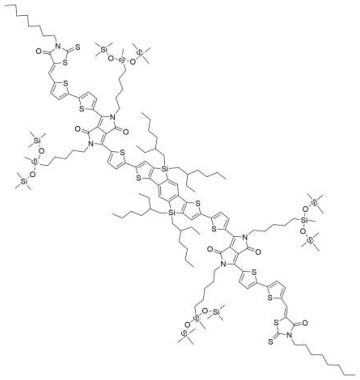 **LGC-D118**	Spin-coating	2-methyl tetrahydro furan	0.82×10^6, 2.60, -5.11±1.58 (*p*-channel)	Glass/Au-Ni/**LGC-D118**/CYTOP/Al	Under N_2	Lim *et al.*[9]
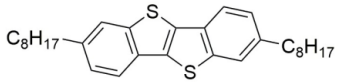 **C_8-BTBT**	Spin-coating	Cyclohexanone	10^7, 4.6, -7.0±1.9 (*p*-channel)	Glass/PVP/Au-Cr/**C_8BTBT**/CYTOP/Al	Vacuum	Sanda *et al.* [10]
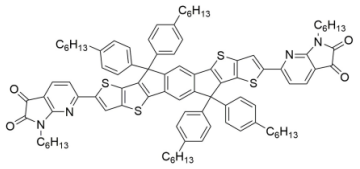 **IDTT-IDD-N**	Spin-coating	Ethyl acetate	2.48×10^7, 1.49, -29.5 (*p*-channel)	Si/SiO_2/OTS/**IDTT-IDD-N**/Au	Vacuum	Zhang *et al.*[11]

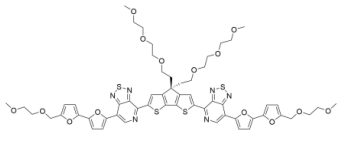 **4**	Spin coating	Ethyl acetate	10^3, 10^{-5}, NA (*p*-channel)	Si/SiO_2/HMDS/**4**/Au	Vacuum	Henson *et al.*[12]
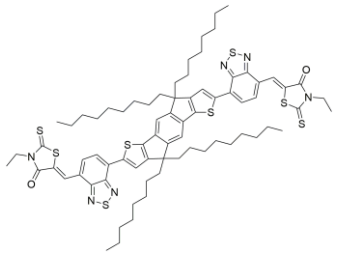 **O-IDTBR**	Blade-coating	Eucalyptol	$>10^5$, 0.37-0.91, 38.8 (*n*-channel)	Glass/Au/**O-IDTBR**/CYTOP CTL-809M/Al	Under N_2	Corzo *et al.* [13]

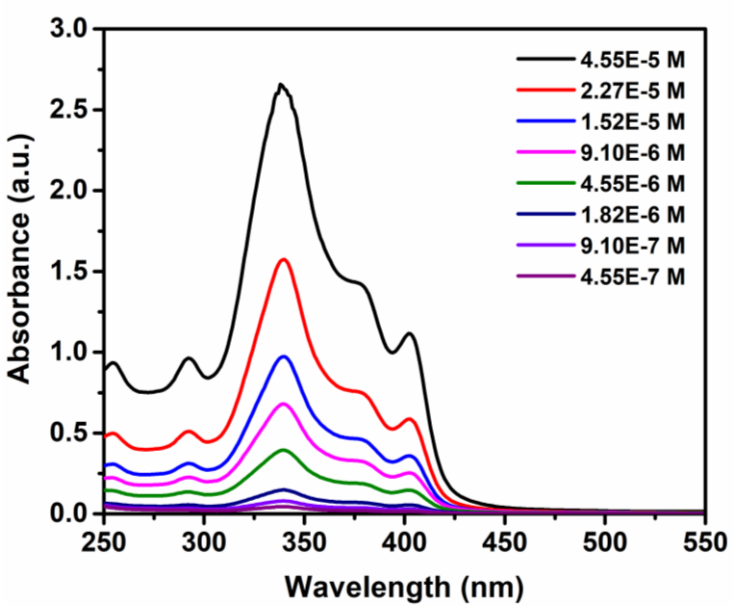

Figure S1. Optical absorption of standard **β,β'-C$_{12}$-TIFDMT** solutions (4.55×10^{-7}–4.55×10^{-5} M) in chloroform. Based on the absorbance values recorded at the molecular absorption maximum (λ_{max} = 338 nm) at different concentrations, a calibration curve (shown in Figure 2(a)) was derived.

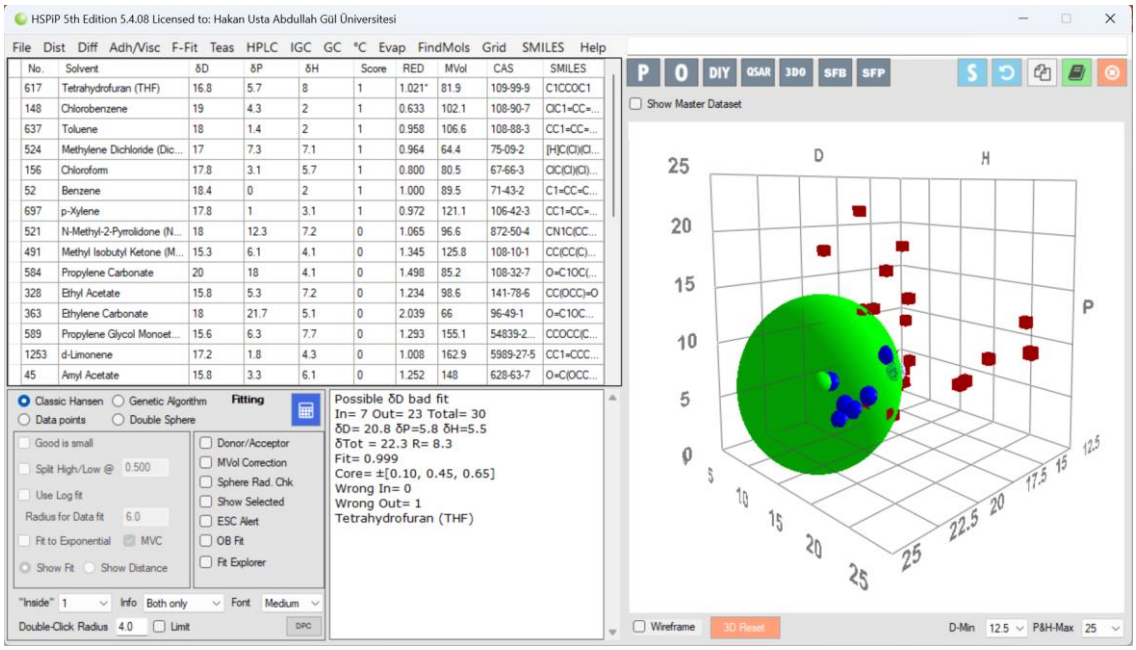

Figure S2. Hansen solubility sphere, parameters, and the fitting accuracy of **β,β'-C$_{12}$-TIFDMT** as determined by using the classic Hansen algorithm in the HSPiP Program (*5th Edition Version 5.4.08*) with a solubility limit of 2 g/L. The Hansen solubility parameters (δ_D, δ_P, δ_H, and R_0) are in MPa$^{1/2}$, the bad (23) and the good (7) solvents are shown in the 3D Hansen solubility solubility space with the red and blue spheres, respectively.

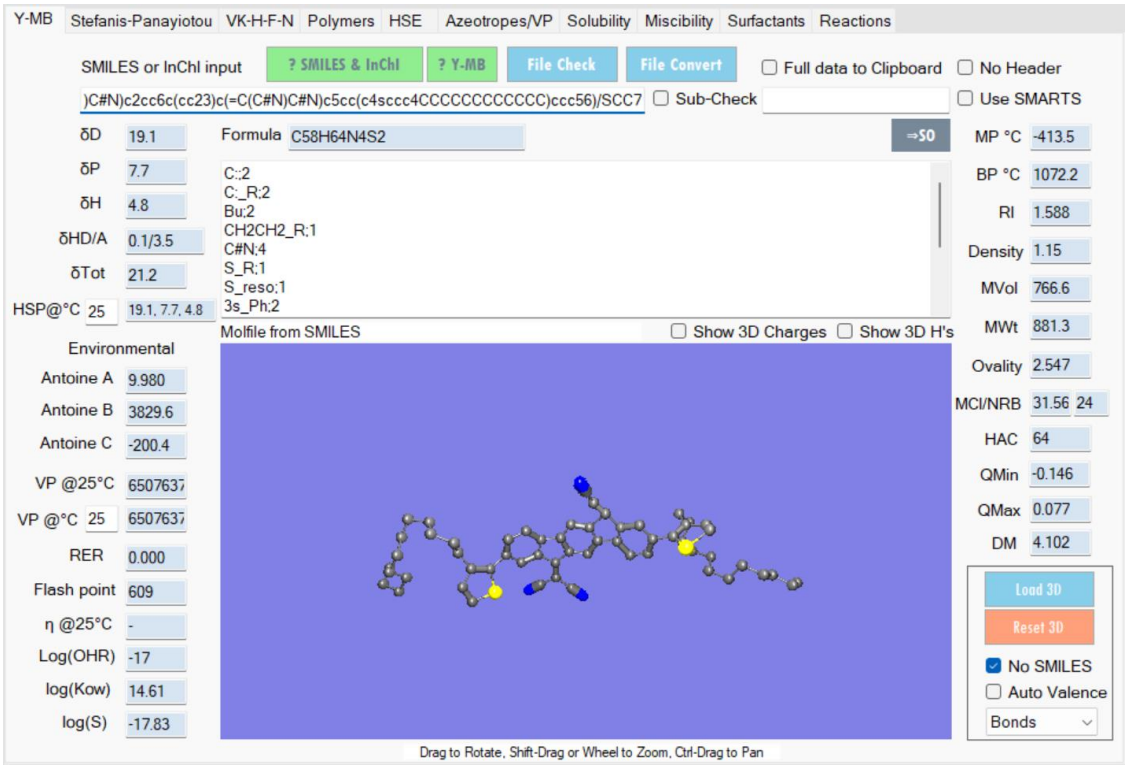

Figure S3. Hansen solubility parameters calculated for **β,β'-C_{12}-TIFDMT** by group contribution methodology in the HSPiP software (*5th Edition Version 5.4.08*) with DIY and Y-MB modules using simplified molecular-input line-entry system (SMILES).

Table S2. The calculation of **β,β'-C_{12}-TIFDMT** mole fraction in varied solvents based on the maximum solubilities measured and the squared interaction distance (Ra^2) between **β,β'-C_{12}-TIFDMT** and the solvent HSPs in the 3D Hansen solubility space.

Solvent	Solvent Density (g/mL)	Solvent Molecular Weight (g/mol)	Max. Solubility (g/L)	Semiconductor Molecular Weight (g/mol)	Semiconductor Mole Fraction	Ra	(Ra)2
Acetone	0.791	58.08	0.05	879.19	4.17576E-06	11.65	135.7225
Acetonitrile	0.786	41.05	0	879.19	0	16.43	269.9449
n-Amyl Acetate	0.87	130.18	0.16	879.19	2.72302E-05	10.32	106.5024
Benzene	0.874	78.11	2.01	879.19	0.000204277	8.3	68.89
1-Butanol	0.81	74.12	0.1	879.19	1.04079E-05	14.08	198.2464
t-Butyl Alcohol	0.775	74.12	0.03	879.19	3.2634E-06	14.51	210.5401
Chloroform	1.492	119.38	6.9	879.19	0.000627562	6.58	43.2964
Cyclohexane	0.779	84.16	0.08	879.19	9.8304E-06	11.21	125.6641
Diethyl Ether	0.706	74.12	0.04	879.19	4.77646E-06	12.96	167.9616
Dimethyl Sulfoxide (DMSO)	1.1	78.13	0	879.19	0	12.54	157.2516
1,4-Dioxane	1.034	88.11	1.11	879.19	0.000107572	8.47	71.7409
Ethanol	0.79	46.07	0	879.19	0	17.38	302.0644
Ethyl Acetate	0.902	88.11	0.13	879.19	1.44435E-05	10.15	103.0225
Ethylene Carbonate	1.32	88.06	0	879.19	0	16.86	284.2596
Ethylene Glycol	1.11	62.07	0	879.19	0	22.47	504.9009
Hexanes	0.659	86.18	0.05	879.19	7.43713E-06	14.25	203.0625
d-Limonene	0.84	136.23	0.3	879.19	5.5336E-05	8.32	69.2224
Methanol	0.791	32.04	0.03	879.19	1.38215E-06	21.75	473.0625
Methyl Iso-Butyl Ketone (MIBK)	0.801	100.16	0.14	879.19	1.99112E-05	11.09	122.9881
N-Methyl-2-Pyrrolidone (NMP)	1.028	99.13	0.5	879.19	5.48372E-05	8.74	76.3876
Methylene Chloride	1.325	84.93	4.9	879.19	0.000357111	7.91	62.5681
N,N-Dimethyl Formamide (DMF)	0.944	73.09	0.13	879.19	1.14483E-05	11.92	142.0864
2-Propanol	0.785	60.1	0	879.19	0	14.79	218.7441
Propylene Carbonate	1.204	102.09	0.05	879.19	4.82216E-06	12.38	153.2644
Propylene Glycol Monoethyl Ether Acetate	0.97	132.16	0.08	879.19	1.23974E-05	10.64	113.2096
Tetrahydrofuran	0.889	72.11	5.3	879.19	0.000488736	8.38	70.2244
Toluene	0.865	92.14	6.7	879.19	0.000811095	7.93	62.8849
Xylene	0.861	106.17	5	879.19	0.00070078	8.35	69.7225
Chlorobenzene	1.106	112.56	7.3	879.19	0.000844311	5.24	27.4576
Cyclopentanone	0.951	84.12	0.79	879.19	7.94746E-05	8.42	70.8964

Theoretical calculation of the intercept in the Hansen-adapted Scatchard-Hildebrand regular solution theory equation (1):

$$-\ln x_{OSC} = \frac{v_{OSC}}{RT}\Phi_{solv.}{}^{2}R_a{}^{2} + \frac{\Delta H_{fus}}{R}\left(\frac{1}{T} - \frac{1}{T_{mp-OSC}}\right) \quad (1)$$

By using the thermal properties of the enthalpy of fusion (ΔH_{fusion} = 36.45 kJ/mol) and the melting temperature ($T_{mp\text{-}OSC}$ = 504.30 K) for **β,β'-C$_{12}$-TIFDMT** (Figure S4),[14] the intercept in equation (1) is calculated to be 6.01. Note that the melting process at 504.30 K leads to a fully isotropic liquid phase, as visually confirmed through conventional melting point measurement. The end-set of the melting temperature is taken as it represents the completion of the melting process.

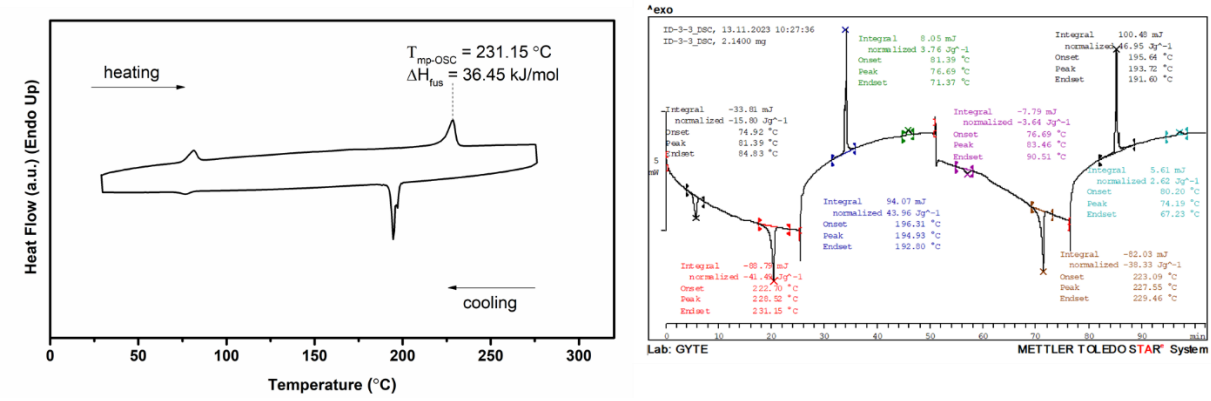

Figure S4. Differential scanning calorimetry scan of **β,β'-C$_{12}$-TIFDMT** at a temperature ramp of 10 °C min^{-1} under N_2 and the raw data from the instrument.

Table S3. The potential green solvents with Hansen solubility parameters (δ_D, δ_P, δ_H in $MPa^{1/2}$) and the corresponding specific **β,β'-C_{12}-TIFDMT**-solvent interaction distance ($R_a = (4\Delta\delta_D^2 + \Delta\delta_P^2 + \Delta\delta_H^2)^{1/2}$ in $MPa^{1/2}$, in which $\Delta\delta$ for a specific Hansen parameter is "$\delta_{OSC} - \delta_{solvent}$").

	Green Solvent	CAS Number	δ_D	δ_P	δ_H	R_a
1	Water	7732-18-5	15.5	16.0	42.3	39.6
2	Pentyl Acetate	628-63-7	15.8	3.3	6.1	10.3
3	Diethyl Carbonate	105-58-8	15.1	6.3	3.5	11.6
4	Anisole	100-66-3	17.8	4.4	6.9	6.3
5	Dimethyl Carbonate	616-38-6	15.5	8.6	9.7	11.7
6	Butyl Acetate	123-86-4	15.8	3.7	6.3	10.2
7	2-Methylanisole	578-58-5	18.3	4.7	4.8	5.2
8	Isobutyl Acetate	110-19-0	15.1	3.7	6.3	11.6
9	Isopropyl Acetate	108-21-4	14.9	4.5	8.2	12.2
10	2-Methyltetrahyrofuran	96-47-9	16.8	4.8	4.6	7.9
11	Cyclohexanone	108-94-1	17.8	8.4	5.1	6.6
12	Dimethyl Succinate	106-65-0	16.1	7.7	8.8	10.1
13	Diethyl Succinate	123-25-1	16.2	6.8	8.7	9.8
14	Methyl Oleate	112-62-9	16.2	3.8	4.5	9.5
15	Ethoxybenzene	103-73-1	18.4	4.5	4.0	5.2
16	Benzyl Alcohol	100-51-6	18.4	6.3	13.7	9.5
17	Cyclohexanol	108-93-0	17.4	4.1	13.5	10.6
18	Diethylene Glycol	111-46-6	16.6	12.0	19.0	17.0
19	Dimethyl Adipate	627-93-0	16.3	6.8	8.5	9.5
20	Triacetin	102-76-1	16.5	4.5	9.1	9.4
21	Triethylene Glycol	112-27-6	16.0	12.5	18.6	17.5

Table S4. The transistor characteristics of p^{++}-Si/SiO_2/PS-brush(M_n = 5 kDa)/**β,β'-C_{12}-TIFDMT**/Au OFET devices having the semiconductor layers processed from anisole, 2-methylanisole, ethoxybenzene, and 2-methyltetrahydrofuran. The average electron mobilities given for each condition are based on at least ten different OFET devices measured.

Green Solvent	**rpm**	**Temperature (°C)**	**μ_{avg} (μ_{max}) ($cm^2V^{-1}s^{-1}$)**	**I_{on}/I_{off}**	**V_T (V)**
Anisole	1500	170	3.87×10^{-3} (6.72×10^{-3})	10^3-10^4	11
		190	0.064 (0.178)	10^6-10^7	2
		200	0.064 (0.122)	10^6	24
	1700	170	0.0706 (0.176)	10^5	10
		190	0.080 (0.155)	10^6-10^7	7
		200	0.032 (0.085)	10^6	10
	2000	170	0.03755 (0.0575)	10^5	18
		190	0.049 (0.136)	10^5	21
		200	0.056 (0.126)	10^5-10^6	33
2-Me-Anisole	1500	170	2.65×10^{-3} (3.98×10^{-3})	10^3-10^4	20
		190	3.81×10^{-3} (8.87×10^{-3})	10^5	15
		200	0.018 (0.022)	10^4-10^5	36
	1700	170	0.011 (0.033)	10^5	7
		190	0.028 (0.052)	10^5	18
		200	0.030 (0.048)	10^6	8
	2000	170	4.00×10^{-3} (9.029×10^{-3})	10^5	17
		190	0.051 (0.125)	10^5	27
		200	0.035 (0.101)	10^6	24

Green Solvent	Rpm	Temperature (ºC)	μ_{avg} (μ_{max}) ($cm^2V^{-1}s^{-1}$)	I_{on}/I_{off}	V_T (V)
Ethoxybenzene	1500	170	1.28×10^{-3} (4.94×10^{-3})	10^4-10^5	13
		190	0.030 (0.060)	10^5-10^6	27
		200	0.022 (0.029)	10^5	28
	1700	170	2.24×10^{-3} (3.76×10^{-3})	10^3-10^4	21
		190	0.040 (0.078)	10^6	15
		200	0.014 (0.029)	10^6	12
	2000	170	4.38×10^{-4} (6.72×10^{-4})	10^2-10^4	20
		190	0.052 (0.089)	10^5-10^6	18
		200	0.030 (0.064)	10^5-10^6	29
2-Me-THF	1500	170	1.58×10^{-3} 3.50×10^{-3}	10^4-10^5	16
		190	6.18×10^{-3} (9.35×10^{-3})	10^5	15
		200	0.013 (0.015)	10^5	14
	1700	170	0.035 (0.089)	10^6	22
		190	0.045 (0.094)	10^6	13
		200	0.082 (0.116)	10^6	13
	2000	170	0.122 (0.192)	10^5-10^6	9
		190	0.028 (0.068)	10^6	15
		200	0.038 (0.059)	10^6	21

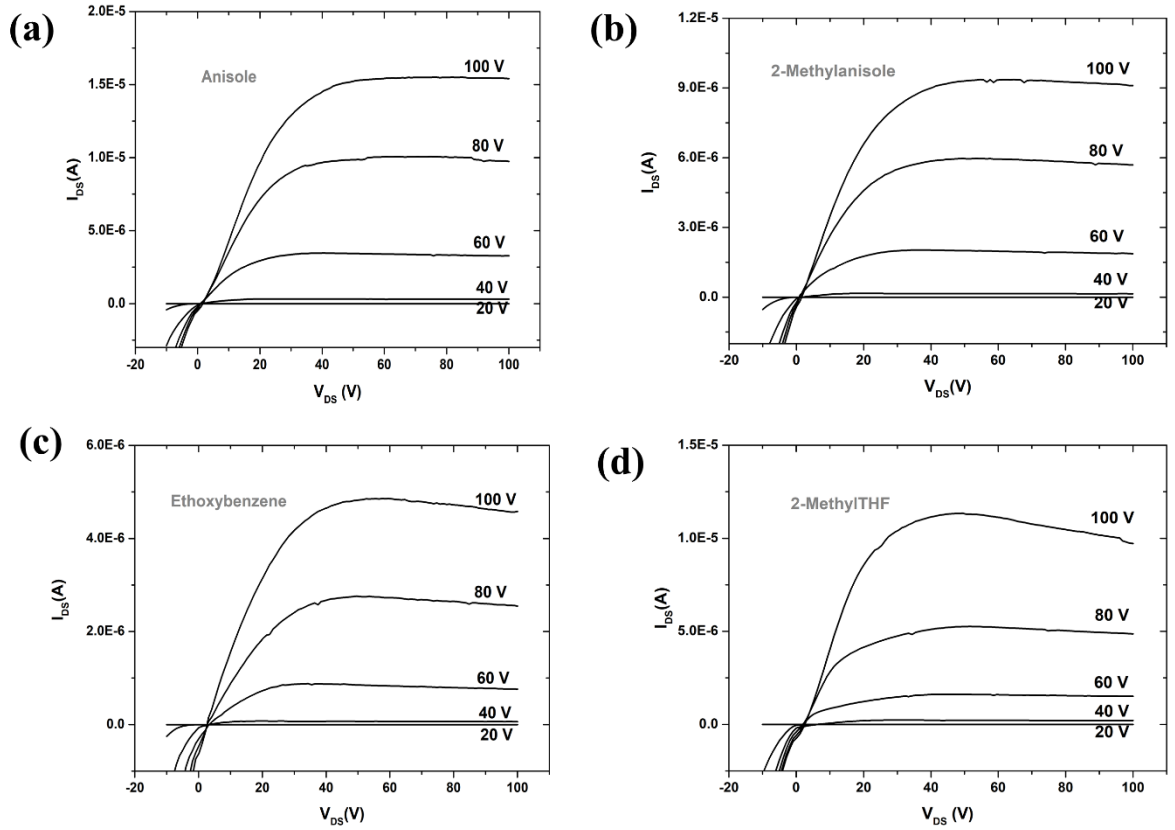

Figure S5. The (*n*-channel) output plots for the p^{++}-Si/SiO_2/PS-brush(M_n = 5 kDa)/**β,β'-C_{12}-TIFDMT**/Au OFET devices, having the semiconductor layers processed from anisole (a), 2-methylanisole (b), ethoxybenzene (c), and 2-methyltetrahydrofuran (d).

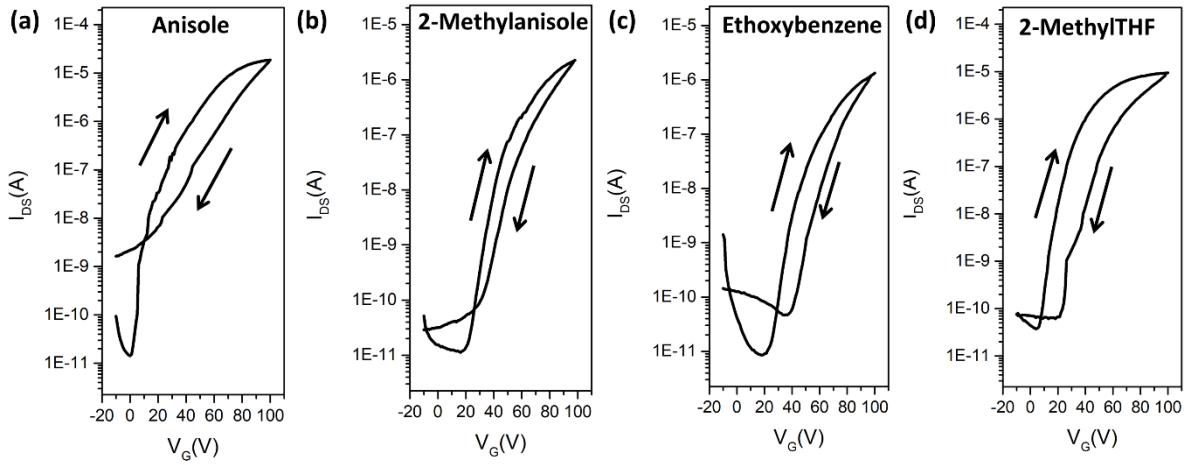

Figure S6. Forward and backward transfer characteristics of the p^{++}-Si/SiO_2/PS-brush(M_n = 5 kDa)/**β,β'-C_{12}-TIFDMT**/Au OFET devices having the semiconductor layers processed from anisole (a), 2-methylanisole (b), ethoxybenzene (c), and 2-methyltetrahydrofuran (d). Channel width and length were 1000 μm and 80 μm, respectively, for all devices.

REFERENCES

[1] D. Ho, J. Lee, S. Park, Y. Park, K. Cho, F. Campana, D. Lanari, A. Facchetti, S. Y. Seo, C. Kim, A. Marrocchi, and L. Vaccaro, "Green solvents for organic thin-film transistor processing" *J. Mater. Chem. C* **8**, 5786–5794 (2020).

[2] D. H. Harris, S. Brixi, B. S. Gelfand, B. H. Lessard, and G. C. Welch, "A N-H functionalized perylene diimide with strong red-light absorption for green solvent processed organic electronics" *J. Mater. Chem. C* **8**, 9811–9815 (2020).

[3] Y. Lee, D. Ho, F. Valentini, T. Earmme, A. Marrocchi, L. Vaccaro, and C. Kim, "Improving the charge transport performance of solution-processed organic field-effect transistors using green solvent additives" *J. Mater. Chem. C* **9**, 16506–16515 (2021).

[4] M. Lee, S. Yun, D. Ho, T. Earmme, A. Marrocchi, L. Vaccaro, and C. Kim, "Green solvent-processed complementary-like inverters based on ambipolar organic thin-film transistors" *J. Ind. Eng. Chem.* **105**, 231–237 (2022).

[5] H. Opoku, B. Nketia-Yawson, E. S. Shin, and Y. Y. Noh, "Controlling organization of conjugated polymer films from binary solvent mixtures for high performance organic field-effect transistors" *Org. Electron.* **41**, 198–204 (2017).

[6] H. Opoku, B. Nketia-Yawson, E. S. Shin, and Y. Y. Noh, "Organic field-effect transistors processed by an environmentally friendly non-halogenated solvent blend" *J. Mater. Chem. C* **6**, 661–667 (2018).

[7] S. Yun, A. Marrocchi, L. Vaccaro, and C. Kim, "Effects of solution-shearing process parameters on charge carrier mobility in green solvent-processed organic field-effect transistors" *Synth. Met.* **291**, 117209 (2022).

[8] S. H. Hong, D. W. Kim, and S. Y. Park, "Aqueous-alcohol-processable indolo[3,2-b]indole-based crystalline small molecules for organic field effect transistors with oligo(ethylene glycol) side chains" *Dye. Pigment.* **211**, 111093 (2023).

[9] B. Lim, H. Sun, J. Lee, and Y. Y. Noh, "High performance solution processed organic field effect transistors with novel diketopyrrolopyrrole-containing small molecules" *Sci. Rep.* **7**, 1–8 (Springer US, 2017).

[10] S. Sanda, R. Nakamichi, T. Nagase, T. Kobayashi, K. Takimiya, Y. Sadamitsu, and H. Naito, "Effect of non-chlorinated solvents on the enhancement of field-effect mobility in dioctylbenzothienobenzothiophene-based top-gate organic transistors processed by spin coating" *Org. Electron.* **69**, 181–189 (2019).

[11] G. Zhang, W. Zhou, M. Kim, M. Sun, H. Lu, L. Qiu, K. Cho, and Y. Ding, "Acceptor-donor-acceptor molecule processed using polar non-halogenated solvents for organic field-effect transistors" *J. Mater. Chem. C* **8**, 6496–6502 (2020).

[12] Z. B. Henson, P. Zalar, X. Chen, G. C. Welch, T. Q. Nguyen, and G. C. Bazan, "Towards environmentally friendly processing of molecular semiconductors" *J. Mater. Chem. A* **1**, 11117–11120 (2013).

[13] D. Corzo, D. Rosas-Villalva, A. C, G. Tostado-Blázquez, E. B. Alexandre, L. H. Hernandez, J. Han, H. Xu, M. Babics, S. De Wolf, and D. Baran, "High-performing organic electronics using terpene green solvents from renewable feedstocks" *Nat. Energy* **8**, 62–73 (2023).

[14] A. Can, İ. Deneme, G. Demirel, and H. Usta, "Solution-Processable Indenofluorenes on Polymer Brush Interlayer: Remarkable N-Channel Field-Effect Transistor Characteristics under Ambient Conditions" *ACS Appl. Mater. Interfaces* **15**, 41666–41679 (2023).